Compressed Sensing Image Reconstruction for CASA

Jonas Schwammberger

Today

Abstract

Solar Flares Abstract

Contents

1 Reconstruction from under-sampled Measurements

In Signal Processing, continuous signals are represented with discrete samples. A digital recording of music, an image of a tree, or the measured velocity of a particle, all are discrete samples of continuous signals. The Nyquist-Shannon sampling rate tells us how many samples are needed to fully represent a signal: A signal which contains at most frequency f should be sampled with a frequency higher than $2f$. For example if we record a piece of music where the highest tone is at 20kHz, sampling rate should be more than 40kHz. Then, the music piece gets recorded above the Nyquist-Shannon sampling rate. It is fully sampled and there is exactly one continuous signal(with maximum frequency f) which fits the measurement.

The Nyquist-Shannon sampling rate is not always achievable: Samples may be expensive to acquire, corrupted by noise, or incomplete by the nature of the measurement instrument. In this case we are dealing with under-sampled measurements. Many possible signals fit the measurement and from the measurement alone, we cannot distinguish the true signal from all possibilities.

With the Theory of Compressed Sensing[5][6] however, we can use prior information about the signal and find the most likely candidate from all possibilities. Under the right conditions, the most likely candidate is guaranteed to be the true signal. With the Theory of Compressed Sensing, we exploit prior information to reconstruct the true signal from under-sampled measurements.

In this project, the Theory of Compressed Sensing gets applied to the image reconstruction problem of interferometers.

In this project, a proof of concept Compressed Sensing reconstruction algorithm was developed and implemented in the Common Astronomy Software Application(CASA). Performance was compared to CLEAN and on VLA measurements of the G55 Supernova Remnant.

1.1 Image Reconstruction for Radio Interferometers

Measure arrival time differences of photons.

In small field of view, it each antenna pair measures approximately a Fourier Component. Phase and Amplitude. measurements.

Only small field of view gets discussed here.

It is called Visibility

If the interferometer would fully sample the Fourier space, the inverse Fourier Transform would produce the image. Since it is under-sampled, the image can be calculated, but is ”dirty”, corrupted by the instrument. The task is to reconstruct the true image from under-sampled Fourier measurements.

The CLEAN class of algorithms[1][2][3][4] are used to reconstruct the image and is the de-factor standard. The prior is a fixed part of the algorithm. Fixed prior about the image.

New instruments like SKA produce new effects. As our knowledge of radio images changes, we want to change the prior of the reconstruction algorithm.

Compressed Sensing is a generalization of CLEAN, prior can be exchanged. With compressed Sensing, A reconstruction algorithm that can change the prior according to what we know.

Antenna beam pattern. Possible super resolution: Structures smaller than the beam size of the antennas.

1.2 Deconvolution of the Dirty Image

A way of modelling the reconstruction problem is in form of a deconvolution. The inverse Fourier Transform computes an image, but the image is ”dirty”, corrupted by effects of under-sampling, beam patterns of the antennas etc.

Fourier Transform produces the dirty image I_{dirty}. It is modified by instrumental effects from under-sampling and antenna beam-pattern. The instrumental effects can be modelled

If the interferometer could sample all Visibilities, then the Fourier Transform would produce the observed image. However, since there are a limited number of antenna pairs, we measure the same limited number of Visibilities. The measurement is under-sampled and the image of the Fourier Transform is ”dirty”. The undersampling convolves the observed image with a point spread function(PSF). The task is to deconvolve the image and remove the effects of undersampling (1.1).

$$x \star PSF + N = I_{dirty} \tag{1.1}$$

the PSF models the instrumental effects of undersampling, antenna beam patterns. The point spread function models the instrument effects. The task is now to deconvolve the image in a noisy environment. .

Equation (1.1) is an ill posed problem::

- It is unknown if a solution exists
- There may be many solutions
- a small change in the measurement may lead to very different solutions

CASA produces a the I_{dirty} image and the PSF.

1.3 Approximation with CLEAN

The prior of CLEAN

Fixed in the algorithm

It works as an approximation of the original problem. It greedily minimizes the objective (1.2). Note that the L0 norm[1] acts as the indicator[2] function.

$$\underset{x}{minimize} \ \|I_{dirty} - x \star PSF\|_2^2 + \ \|x\|_0 \tag{1.2}$$

Regularization term, minimum, non-convex function (It may have local minima). The L0 ”norm” makes this problem for non-convex: It may it is in NP-Hard. There exist optimizer like Matching Pursuit that approximate the solution well enough for practice.

but CLEAN does not minimize to an optima, it stops early. Hard to analyse how close the current solution is to the true minimum.

Convolution with antenna beam-pattern.

CLEAN does a greedy approximation of the deconvolution problem, and assumes the resulting image consists out of a few point sources. The question remains, how close the CLEAN approximation is to the true image?

[1] This is a common abuse of notation in Compressed Sensing literature: The ”L0 norm” is not a norm.
[2] For the L0 norm to work we need to define $0^0 = 0$

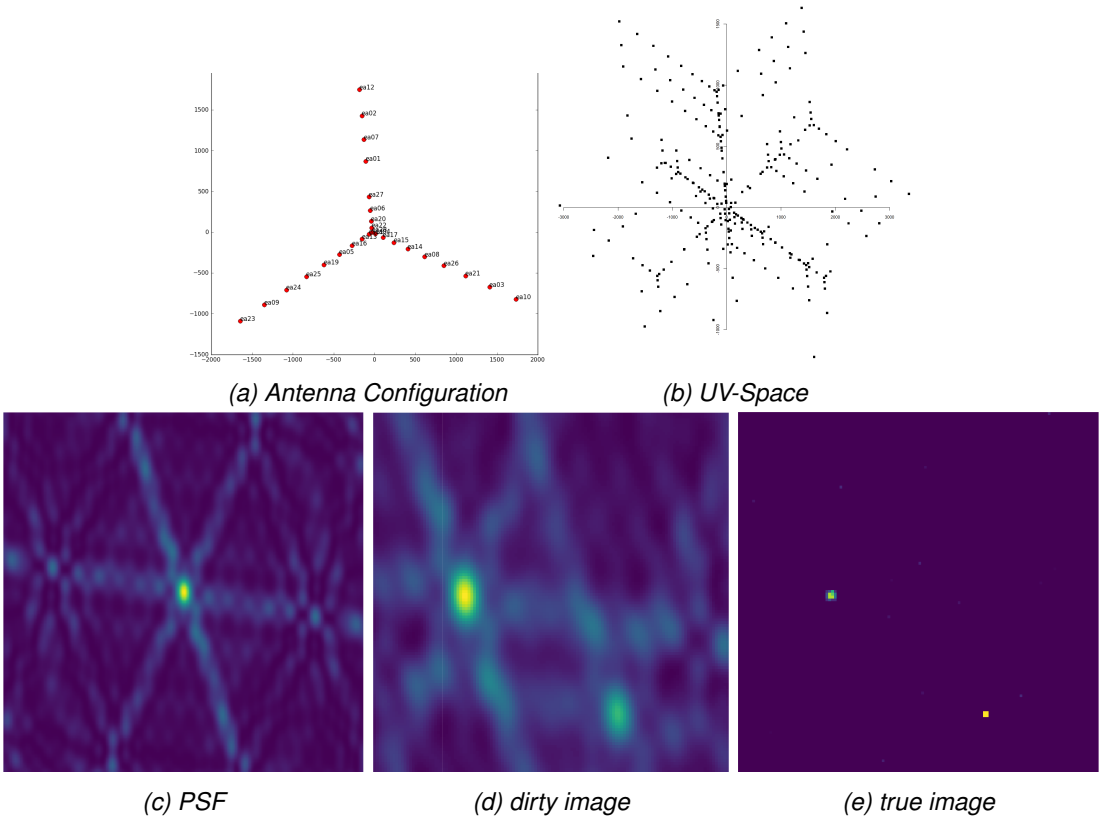

(a) Antenna Configuration *(b) UV-Space*

(c) PSF *(d) dirty image* *(e) true image*

Figure 1: Deconvolution Problem VLA: Retrieve the true image when only PSF and dirty image are known

If the true image consists out of a few point sources, CLEAN produces a good approximation. Extended emissions however get approximated by a large number of faint point sources. The peak of extended emissions are generally lower than of point sources. CLEAN has more trouble distinguishing extended sources from noise. Future interferometers like MeerKAT will become more sensitive to fainter sources. The reconstruction task for new instruments may contain more faint and extended sources. Ideally, we would modify the regularization of CLEAN and explicitly model the new effects. Sadly, the regularization is a fixed part of the CLEAN algorithm.

1.4 CLEAN as Compressed Sensing Image Reconstruction

An image reconstruction algorithm in the Compressed Sensing Framework consists of three parts:

- A prior function $p()$.
- An optimization algorithm.
- An objective with a data and regularization term.

CLEAN is a Compressed Sensing Reconstruction algorithm with specific choices for prior, optimization algorithm. and objective. The prior $p()$ in CLEAN is the L0 ”norm”, Matching Pursuit as the optimization algorithm. The objective from CLEAN needs a additional parameter λ. [which represents the trade-off between deconvolution and regularization.] the more noisy it is, the more regularization is needed. We arrive at the similar (1.3).

$$\underset{x}{minimize} \ \|D_{dirty} - x \star PSF\|_2^2 \ + \ \lambda \, p(x) \tag{1.3}$$

All that was changes was an additional parameter λ, so why would one want to do this? Applying non-convex optimization techniques, Theoretical guarantees of compressed Sensing. Replacing $p()$ with anything else

Now we can minimize (1.3) with non-convex optimization techniques, we can analyse how calculate lower limits for the objective.

We assume x assumes the x contains a few point sources. In Compressed Sensing terminology, it assumes x is sparse in image space. Since x is already an image.

Compressed sensing reconstruction is able to reconstruct the observation even from undersampled measurements. Even though shannon-nyquist theorem is higher.

The guarantees of Compressed Sensing Reconstruction: Incoherent from the measurement space and sparse space is sparse.

Incoherence is easy. Interferometers measure in the Fourier space(This is an approximation for small field of view imaging. The approximation breaks apart in wide field of view). The image space is maximally incoherent from the Fourier space. Intuitively, A change in a single pixel will change all fourier components. A change in a single fourier component, changes all pixels.

maximize the information gained for each element in the sparse space.

The sparse space is here to distinguish true image from unlikely candidates. It models our prior knowledge.

Then, one can reconstruct the true image from undersampled measurements. How many measurements are needed? that depends on how sparse it is.

Taking again CLEAN as an example, if we know the image contains only one point source, we can locate it with only a few Visibilities. However if the image contains many point sources located closely together, we need more Visibilities.

The average case analysis is not trivial,

The prior and the optimization algorithm are disconnected and the prior $p()$ can be replaced for example with the L2 norm.

2 Inverse Problem for wide Field of View Imaging

So far the small Field of View inverse problem has been introduced where each antenna pair measures a Visibility of the sky brightness distribution. This leads to the small Field of View measurement equation (2.1). It is identical to the two dimensional Fourier Transform. In practice the Fast Fourier Transform (FFT) is used, since it scales with $n\,log(n)$ instead of n^2 pixels.

$$V(u,v) = \int\int x(l,m)e^{2\pi i(ux+vy)}dldm \tag{2.1}$$

For wide Field of View imaging, two effects break the two dimensional Fourier Transform relationship: Non-coplanar Baselines and the celestial sphere which lead to the measurement equation (2.2). Note that for small Field of View $1-x^2-y^2 \ll 1$, and (2.2) reduces to the 2d measurement equation (2.1).

$$V(u,v,w) = \int\int \frac{X(x,y)}{\sqrt{1-x^2-y^2}} e^{2\pi i(ux+vy+w\sqrt{1-x^2-y^2})}dxdy \tag{2.2}$$

Non-coplanar Baselines lead to a third component w for each Visibility. Figure 2 shows the the u v and w coordinate system. w is essentially the pointing direction of the instrument. The UV-Plane is the projection of the antennas on a plane perpendicular to the pointing direction. Which point in the UV-Plane get sampled and what w component it has depends on the pointing direction. If the instrument points straight up, the UV-Plane is a tangent to earth's surface, and the w term compensates for earth's surface curvature. If however the instrument points at the horizon, the projected UV-Plane gets squashed and w compensates for antennas which lie far behind the UV-Plane. In essence, w is a phase delay that corrects antenna positions in three dimensions. The wide Field of View measurement equation (2.2) would account for the w phase delay, but it breaks the the two dimensional Fourier relationship and the FFT cannot be used. The W-Projection [7] algorithm approximates the effect of the w term restores the two dimensional Fourier relationship.

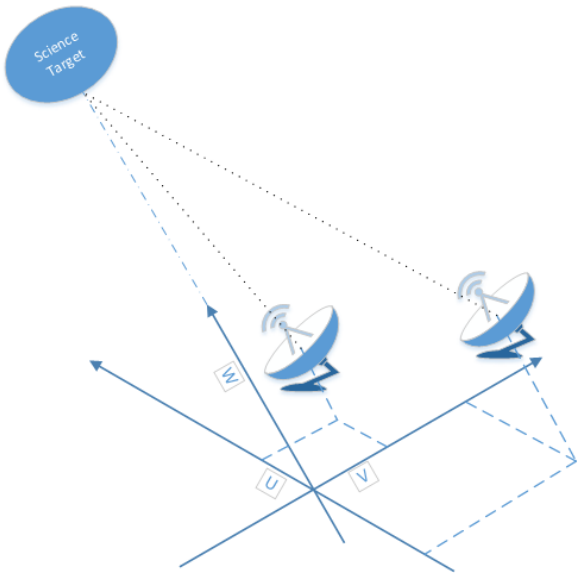

Figure 2: U V and W coordinate space

A-Projection [8]

2.1 Directionally Dependent Effects (DDE)

spread spectrum phenomenon

2.2 Calibration

2.2.1 Self-Calibration

3 Compressed Sensing Image Reconstruction

The Framework Flexibility

A lot of choice in building a reconstruction algorithm. No best

Gurobi[9] was used.constrained optimization.

3.1 Sparseland Prior and Overcomplete Representations

The prior $p()$ can be any function like the LP norm.

We could use L2, but what we mostly want in Compressed Sensing Reconstruction is sparsity. With that, L0 ”norm” is often used.

The L1 relaxation however is practically guaranteed to have the same minimum as the L0 norm and results in a convex objective function. Since Gurobi works better on the L1 relaxation it was chosen for this project.

In practice, sparseland priors (3.1) have been used for Compressed Sensing reconstruction: For our signal x we create a dictionary D. Each entry in D represents a signal part of x. D is potentially a large, but has a finite number entries. However, any x we measure consists only of a few entries of D. This means the coefficients for the signal parts in the dictionary α are all zero except for s entries for all valid x.

$$\begin{aligned} x = D\alpha \qquad x \in \mathbb{R}^n, \alpha \in \mathbb{R}^m, D \in \mathbb{R}^{n*m}, \qquad n \leq m \\ \|\alpha\|_0 = s \qquad s \ll n \leq m \end{aligned} \tag{3.1}$$

In other words, we create a dictionary D in which our signal can be sparsely represented. Together with the L1 norm, the sparseland prior can be thought of as a detector for our signal. Any valid x can be sparsely represented, but noise tends to affect all entries.

In the Compressed Sensing Reconstruction we want to find our x in a noisy environment. The optimization algorithm locates the s significant entries in α and throws away the rest.

Reconstructing an image from measurements is related to lossy image compression. Indeed, we know our image can be compressed in a dictionary D, the same D works well for reconstruction: For example images depicting nature scenes are sparse in the wavelet domain. If x in (3.1) are nature scenes, we can create a Dictionary D of wavelets. A single image x can be represented with a few wavelets, meaning the number of non-zero entries s in α is far lower than the number of pixels n. All that is left to do for compression is save the non-zero entries of α. In the noisy environment, we save the s largest elements of α and save a de-noised image.

Find a dictionary D in which radio can be seen as finding a compression space.

Finding the right sparseland prior is a modelling task. It codes our prior knowledge about radio sources and what they might produce. Sparseland priors are in use by for example with Starlets[10] and Curvelets[11].

Any combination of functions

Sparseland priors naturally lend themselves to overcomplete representations. D has many more rows than columns.

3.2 Choosing the Objective Function

Until now, the objective function was used as a deconvolution. This is not a requirement of Compressed Sensing. It is a design choice.

Different ways of choosing the objective function with a sparseland prior.

There are three different reconstruction objectives: The analysis method, where the image x is minimized directly, the synthesis method where the sparse vector α is minimized, or by in-painting the missing Visibilities V_2.

$$
\begin{aligned}
analysis: \quad & \underset{x}{minimize} \ \|I_{dirty} - x \star PSF\|_2^2 \quad + \lambda \|Px\|_1 \\
synthesis: \quad & \underset{\alpha}{minimize} \ \|I_{dirty} - D\alpha \star PSF\|_2^2 + \lambda \|\alpha\|_1 \\
in-painting: \quad & \underset{V_2}{minimize} \ \left\|I_{dirty} - F^{-1}MV_2\right\|_2^2 \quad + \lambda \left\|PF^{-1}V_2\right\|_1
\end{aligned}
$$

All three objective functions have the same global minimum. Retrieving x for the analysis objective is trivial, or the second and third objective x can be retrieved by $x = D\alpha$ and by $x = F^{-1}V_2$ respectively. [Empirical and theoretical studies have shown an advantage of the analysis objective over the other two [**?**]]. However, depending on the measurement space and prior, an objective might become more practical.

The analysis and in-painting objective require the inverse of the dictionary D^{-1}. It exists for orthogonal transformation like the Haar Wavelet transform and for specialized over-complete dictionaries like starlets. In general, over-complete dictionaries do not have an inverse. The synthesis objective is suited for general dictionaries as it does not use the inverse.

During this project, no reconstruction algorithm was found which uses the in-painting method. Convolutions in image space are equivalent to a multiplication in Fourier Space.

Useful when the Dictionary transformation is defined as a deconvolution.

3.3 Compressed Sensing Reconstruction Algorithms in Astronomy

multiple

3.3.1 PURIFY

Prior: Mixture of Dirac functions and Daubechies Wavelet (DB1 - DB8)

Objective: analysis

Optimizer: SDMM

Dirac is a fancy way of saying ”it is sparse in pixel space”

3.3.2 Vis-CS

Prior: dictionary of gaussians

Objective: Synthesis

Optimizer: Coordinate descent

3.3.3 SASIR

Was chosen because it has an inverse. Multiscale effects included in prior.

Prior: Starlets

Multi scale prior, over complete representation but with a transformation from image space in starlet space.

Objective: synthesis

Optimizer: FISTA

3.4 Implementation In CASA

CASA is a software package built for reconstructing images for VLA.

CASA works in two separate cycles, the major and minor cycle. The major cycle transforms the Visibilities to image space and back using the Fourier Transform. The minor cycle is the deconvolution algorithm, which tries to find the true image from a dirty image and a PSF.

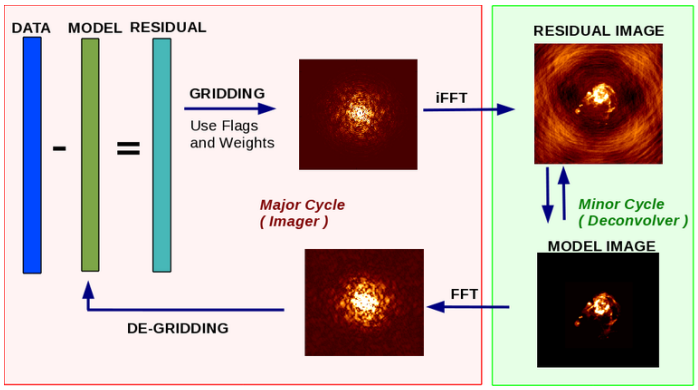

Figure 3: Casa Major Minor Cycle. Source [12]

The first major cycle iteration creates the PSF and the dirty image. Then, several minor cycle deconvolve the dirty image. The major cycle then continues, transforms the deconvolved image back to Visibilities. The major cycle ends by calculating the residual Visibilities from the measurement and the deconvolution. The next major cycle continues by transforming the residual Visibilities. At the end of several major cycle, the model column should contain an approximation of the true visibilities while the residuals should be noise.

In CASA the major cycle is fixed. It was evaluated if it can be modified, but a modification was too time consuming in the context of the project. However CASA allows for the addition of new deconvolution algorithms.

Compressed Sensing Algorithm was implemented as a CASA deconvolver. The Data term of the objective is fixed to be the deconvolution ($D_{dirty}x - \star PSF$).

Major cycle is more expensive to compute than a CLEAN minor cylce.

CLEAN needs potentially many major cycle iterations. A Compressed Sensing Reconstruction would converge to the optimum in one major cylce. Here lies a potential speedup for the Compressed Sensing Reconstruction.

4 Reconstruction for VLA Observations

Compressed Sensing Reconstruction used on two different tasks:

- Center detection on sunburst data
- Reconstruction from incomplete measurements of Supernova Remnant G55

Two different problems. One is the

Structure potentially smaller than the primary beam.

4.1 Sunburst Center Detection

Sub- Primary Beam. CS Objective Function

Figure: Dirty Map Peak, CLEAN, Single Peak Clean, Single Peak CS Reconstruction

Wider Variance

4.2 Reconstruction of Supernova Remnant G55

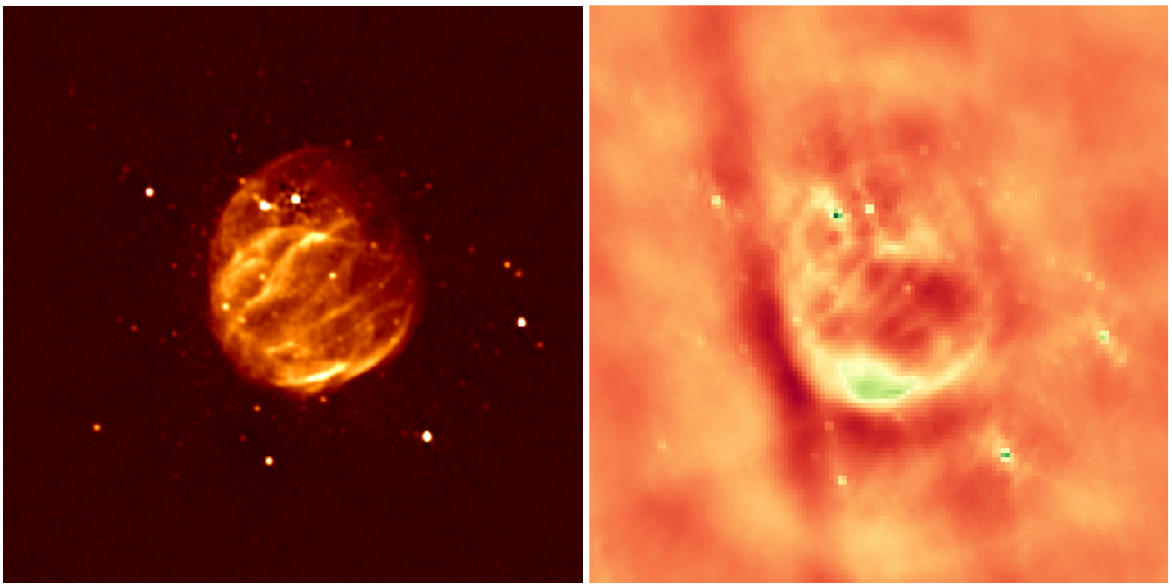

(a) Reconstruction by NRAO. Source:[13] *(b) Dirty Image*

Figure 4: SNR G55 source observed by VLA.

The supernova remnant (SNR) G55 was observed by VLA. 10 seconds of the 8 hour observation is publicly available through the CASA imaging tutorial[14]. 4b is the dirty image calculated from the 10 second observation. The full 8 hours are not readily available. The image 4a is a reconstruction from an unknown VLA observation. The deconvolution algorithm is also unknown. For this project, the reconstructed image is assumed to show the true image of the sky.

4 shows G55 to be a slightly ”egg shaped” extended emission with six strong point sources. Several fainter point sources are inside and around the egg shaped extended emission. The dirty image 4b shows a corrupted

version of G55. The six strong point sources are clearly visible as are the brighter parts of the extended emission. The dirty image also shows a negative ”trench” striking through the image as well as brighter regions around the remnant.

The size of the images 4 is about twice the size of the primary beam (the primary beam is approximately the size of the extended emission). In the real world, wide field imaging would be used. In this project, small field of view imaging was used because it is quicker to compute. It limits the dynamic range of the dirty image, the whole task gets harder.

The CLEAN algorithm gets compared to Compressed Sensing Reconstructions. The parameters of CLEAN were taken from the CASA imaging tutorial[14]. The reconstructed images of Compressed Sensing are constrained to have no negative pixels. Negative pixels are not physically plausible and was shown to improve Compressed Sensing reconstructions for synthetic data[15]. In total six different priors were tested with the analysis objective:

1. No Regularization
2. L1
3. L2
4. L1+L2
5. Total Variation
6. Starlet Transform

The regularization parameter λ needs to be estimated for each prior. The Miller[16] λ estimation was used and is shown in equation (4.1). [Estimation of the noise level e, divided and E]. An approximate solution is needed to define the noise level and the amount of regularization. In this project, the result with no regularization was used for the λ estimation.

This is not an ideal estimation, the image effectively gets reconstructed twice. Other Compressed Sensing Reconstructions approximate x of equation (4.1) by running their optimizer a couple of iterations without regularization, which reduces the computational costs.

$$\lambda \approx e/E \qquad \|I_{dirty} - x \star PSF\|_2^2 \leq e \qquad p(x) \leq E \tag{4.1}$$

Two figures compare the Dirty Image, CLEAN and the Compressed Sensing Reconstrutions. Figure 5 shows the reconstructed images on the same intensity scale. Figure 6 shows the flux profile of a cut through the reconstructed images. The Cut through the remnant is located in the center of the profile image.

CLEAN: CLEAN detects the brightest point sources, but finds only part of the extended emission. The top half of the ”egg” emission is missing. The structures of the remnant are blurred compared to the Compressed Sensing reconstructions. With the parameters of the imaging tutorial, CLEAN models the trench as a region with negative emissions. This is not physically plausible, although the behaviour can be changed with additional parameters. The profile 6 shows that CLEAN accurately reconstructs the flux of the large peaks, although the peaks are wide in comparison.

No Regularization: Detects the Egghead of the remnant and the non-negativity constraint keeps it from modelling the negative trench. It detects the smaller emissions around the remnant, but also detects ”fake” extended emissions. The profile 6 shows two smaller peaks in the center which also appear in 4a as do the two small point sources at the edge of the remnant. However, the dirty image has a rise in flux at the borders of the image, which is likely an artefact of the measurement, considering it does not exist in the NRAO reconstruction 4a.

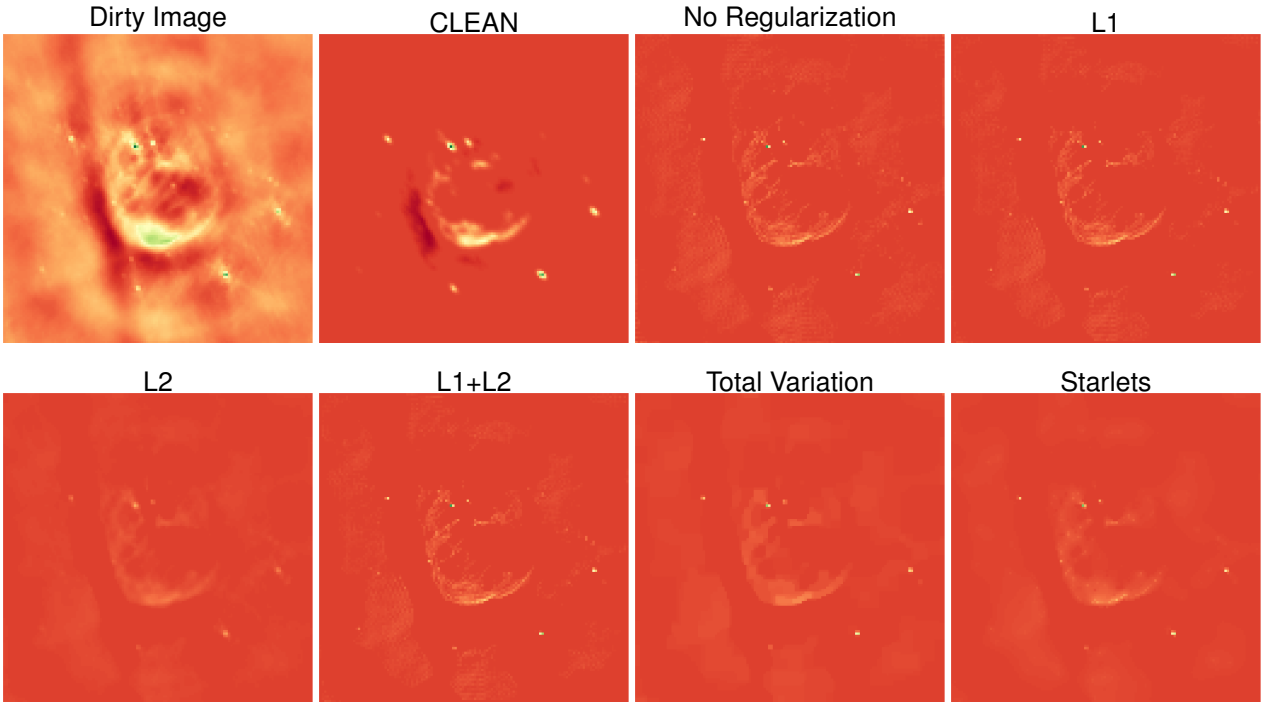

Figure 5: Reconstructed images of CLEAN and the different Compressed Sensing priors.

L1: There is almost no visible difference between no regularization and L1. This is possibly an interaction with the Miller λ estimation, since the result of no regularization was used to estimate the λ of L1. The L1 regularization removes part of the ”fake” extended emission, particularly in the top region, but also a few structures in the center. The peaks in the profile 6 of L1 and no regularization are narrower than CLEAN, although they do not reach the same peak flux. L1 is prone to produce unlikely extended emissions: L1 also tries to approximate extended emissions with a number of faint point sources. This can introduce artefacts like pixel wide holes in extended emissions.

L2: Forces the extended emissions to be more smooth. It also considerably lowers the flux of bright point sources. The profile 6 shows L2 forces the bright peak to widen and lower. The peak is almost as wide as the CLEAN reconstruction. In the remnant center, it smoothers the smaller peaks.

L1+L2: Since L1 does a good job with point sources, but needs to be more continuous for extended emissions, why does one not combine both regularizations? The flexibility of Compressed Sensing Reconstructions allows for it. Sadly, the result is indistinguishable from the L1 regularization. In the dirty image, all pixels are very close to zero (Maximum: 0.0076 in Dirty Image). If the L1 and L2 regularization receive the same λ, the L1 term dominates. If the dirty image would contain pixels much larger than 1, then the L2 term would dominate.

Total Variation: A simple prior that has its origins in image de-noising. The objective is to reduce the gradients over the image. With an infinite λ, the Total Variation forces all pixels of the reconstruction to have the same value. The idea of the prior is to work well for both extended emissions and point sources. It has trouble with point sources inside extended emissions. In the profile, it is clearly visible how Total Variations cuts the peaks inside the remnant.

Starlets: Is a more sophisticated prior which also tries to model both point sources and extended emissions. It locates the point sources accurately. In the profile 6 it also finds the faint point sources in the extended emission. However, it also smoothed out the structure inside the remnant. For the LOFAR instrument, the starlet regularization was able to find smaller structures than the antenna beam-width[17]. The smallest starlet has a $5 * 5$ pixels dimension. For this reconstruction, the antenna beam-width is about two pixels wide. The

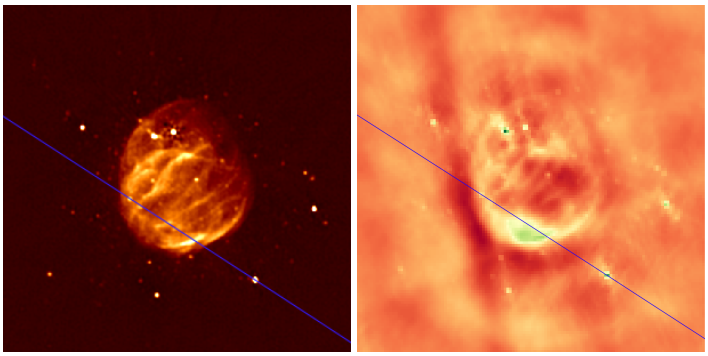

(a) profile cut

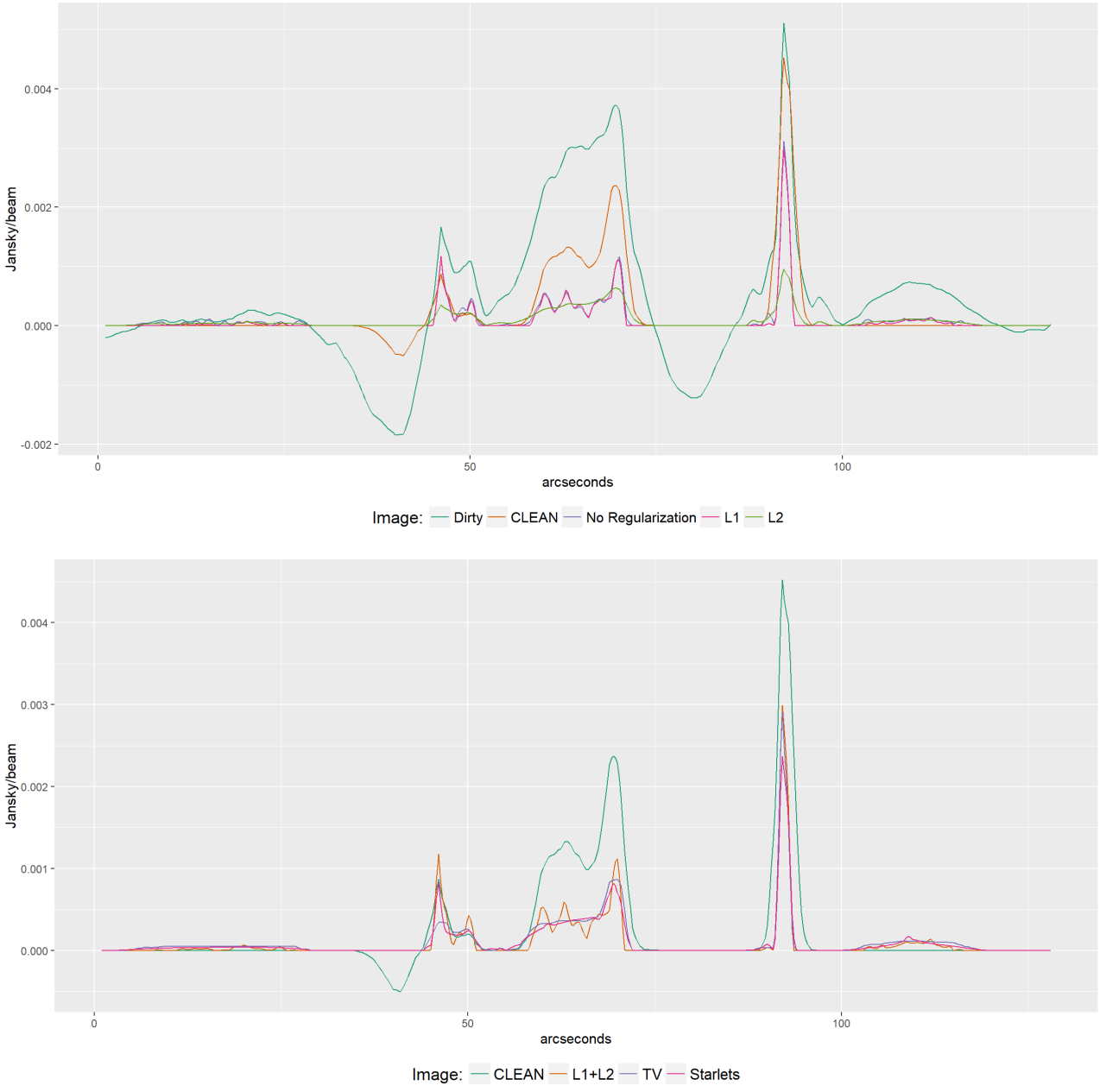

Figure 6: Intensity profile of CLEAN and the different Compressed Sensing Regularizations.

resolution might be too coarse for the starlet regularization.

CLEAN produces the most accurate flux for strong point sources, even though in other reports Total Variation and Starlets reconstructed comparable peak flux to CLEAN [18][15].This is due to the implementation in CASA: The PSF CASA produces does not sum up to one. Convolving an image with the PSF increases the total flux, and naturally a deconvolution decreases the flux. CLEAN is the only algorithm that comes close to the measured flux, because in the last iteration, the reconstructed image gets convolved with the beam pattern (usually a 2d gaussian function), which is also not normalized. If we also convolve the Compressed Sensing reconstructions with the beam pattern (and smear away details), the fluxes become similar.

In this example, the L1 normalization was able to find smaller, plausible structures than CLEAN inside the remnant. Outside the remnant, all Compressed Sensing Reconstructions found ”fake” extended emissions. The L2 and starlet were also expected to find smaller structures. One possible explanation is that the antenna beam-width is about two pixels wide. Any structure smaller than the beam-width is one pixel wide.

For higher resolutions it is expected that L1 introduces more artefacts. The current implementation cannot increase the resolution since it needs a quadratic amount of memory per pixel: The image size of about 128^2 was the maximum which was feasible to solve on a laptop. The convolution operation $x \star PSF$ gets modelled as a matrix-vector product. The matrix therefore has 128^4 entries.

5 Future in Compressed Sensing Reconstruction

The flexibility of Compressed Sensing Reconstructions allows us to change the prior according to our previous knowledge, all while keeping the same objective and optimization algorithm. The prior can be updated as our knowledge changes. It was able to find plausible structures smaller than the antenna beam-width. Using Compressed Sensing Reconstructions gives us theoretical guarantees that, if our prior models the observation well enough, we reconstruct the true image from under-sampled measurements.

A proof of Compressed Sensing Reconstruction was implemented in CASA as a minor cycle deconvolver. It takes the dirty image and point spread function as input and calculates the optimal deconvolution according to the objective. The current implementation has a quadratic memory requirement. It does not scale to any practical image size for VLA observations. New interferometers like MeerKAT will require even larger images. The current implementation is not suited for large scale reconstructions.

Self-calibration is a task which was not covered in this project. Self-calibration aims to reconstruct both the image and the the antenna gain calibration from the same measurements. Here with Compressed Sensing Reconstructions one may be able to apply complex optimization techniques to self-calibration, and find the global optimum of both calibration and reconstructed image.

New interferometers are built with wide field of view imaging in mind, which introduces new measurement effects that a reconstruction algorithm should account for. State of the art Compressed Sensing Reconstructions take the measurements as input and also correct wide field of view effects. Due to the CASA interface, the current implementation is restricted to be in the image space, the effects of wide field of view are currently handled by CASA. The next step is a Compressed Sensing Reconstruction which accounts for the effects of wide field imaging and scales to astronomical image sizes.

References

[1] JA Högbom. Aperture synthesis with a non-regular distribution of interferometer baselines. Astronomy and Astrophysics Supplement Series, 15:417, 1974.

[2] FR Schwab. Relaxing the isoplanatism assumption in self-calibration; applications to low-frequency radio interferometry. The Astronomical Journal, 89:1076–1081, 1984.

[3] JW Rich, WJG De Blok, TJ Cornwell, Elias Brinks, Fabian Walter, Ioannis Bagetakos, and RC Kennicutt Jr. Multi-scale clean: A comparison of its performance against classical clean on galaxies using things. The Astronomical Journal, 136(6):2897, 2008.

[4] Urvashi Rau and Tim J Cornwell. A multi-scale multi-frequency deconvolution algorithm for synthesis imaging in radio interferometry. Astronomy & Astrophysics, 532:A71, 2011.

[5] Emmanuel J Candès, Justin Romberg, and Terence Tao. Robust uncertainty principles: Exact signal reconstruction from highly incomplete frequency information. IEEE Transactions on information theory, 52(2):489–509, 2006.

[6] David L Donoho. Compressed sensing. IEEE Transactions on information theory, 52(4):1289–1306, 2006.

[7] Tim J Cornwell, Kumar Golap, and Sanjay Bhatnagar. The noncoplanar baselines effect in radio interferometry: The w-projection algorithm. IEEE Journal of Selected Topics in Signal Processing, 2(5):647–657, 2008.

[8] S Bhatnagar, TJ Cornwell, K Golap, and Juan M Uson. Correcting direction-dependent gains in the deconvolution of radio interferometric images. Astronomy & Astrophysics, 487(1):419–429, 2008.

[9] Gurobi Optimization. Gurobi optimizer, 2018.

[10] Jean-Luc Starck, Fionn Murtagh, and Mario Bertero. Starlet transform in astronomical data processing. Handbook of Mathematical Methods in Imaging, pages 2053–2098, 2015.

[11] Jean-Luc Starck, David L Donoho, and Emmanuel J Candès. Astronomical image representation by the curvelet transform. Astronomy & Astrophysics, 398(2):785–800, 2003.

[12] National Radio Astronomy Observations. tclean overview, 2016.

[13] National Radio Astronomy Observations. Glowing bubble of an exploded star, 2016.

[14] National Radio Astronomy Observations. Vla casa imaging-casa5.0.0, 2017.

[15] Jason D McEwen and Yves Wiaux. Compressed sensing for radio interferometric imaging: Review and future direction. In Image Processing (ICIP), 2011 18th IEEE International Conference on, pages 1313–1316. IEEE, 2011.

[16] Keith Miller. Least squares methods for ill-posed problems with a prescribed bound. SIAM Journal on Mathematical Analysis, 1(1):52–74, 1970.

[17] Julien N Girard, Hugh Garsden, Jean Luc Starck, Stéphane Corbel, Arnaud Woiselle, Cyril Tasse, John P McKean, and Jérôme Bobin. Sparse representations and convex optimization as tools for lofar radio interferometric imaging. Journal of Instrumentation, 10(08):C08013, 2015.

[18] Hugh Garsden, JN Girard, Jean-Luc Starck, Stéphane Corbel, C Tasse, A Woiselle, JP McKean, Alexander S Van Amesfoort, J Anderson, IM Avruch, et al. Lofar sparse image reconstruction. Astronomy & astrophysics, 575:A90, 2015.

List of Figures

List of Tables

6 Ehrlichkeitserklärung

Hiermit erkläre ich, dass ich die vorliegende schriftliche Arbeit selbstständig und nur unter Zuhilfenahme der in den Verzeichnissen oder in den Anmerkungen genannten Quellen angefertigt habe. Ich versichere zudem, diese Arbeit nicht bereits anderweitig als Leistungsnachweis verwendet zu haben. Eine Überprüfung der Arbeit auf Plagiate unter Einsatz entsprechender Software darf vorgenommen werden.
Windisch, July 29, 2018

Jonas Schwammberger